Fab & Facilities
Materials
Cell Processing
Thin Film
PV Modules
Market Watch

Cell-to-module power loss/gain analysis of silicon wafer-based PV modules

Jai Prakash Singh, **Yong Sheng Khoo**, **Jing Chai**, **Zhe Liu** & **Yan Wang**, Solar Energy Research Institute of Singapore (SERIS), National University of Singapore (NUS), Singapore

ABSTRACT

We are always hearing about champion cells demonstrating efficiencies of 24% or higher, yet only 20 or 21% can be obtained at the module level. Where are all these hard-earned electrons going? Moreover, why should every photon and electron be counted? Cell efficiency is important, but it is *module* efficiency that defines the bottom line of every solar project. This paper will highlight the different loss mechanisms in a module, and how they can be quantified. Once it is known where photons and electrons are lost, it is possible to develop strategies to avoid this happening. In-depth loss-analysis methods for studying various loss mechanisms in a PV module have been developed at SERIS. Using these methods, in combination with various characterization tools/techniques, such as external quantum efficiency (EQE) line scan, electroluminescence imaging, and IV testers, a detailed loss/gain analysis of the cell-to-module process has been carried out and is presented in this paper. The loss/gain analysis is demonstrated using two dominant cell technologies: p-type multicrystalline and n-type monocrystalline cells.

Introduction

In conventional silicon wafer-based PV technology, solar cells are connected in series and encapsulated into PV modules. The interconnection increases the power and voltage, while the encapsulation provides environmental protection for the solar cells. The main purpose of a PV module is to protect the cells from the harsh environment throughout an expected lifetime of 20 to 25 years.

Although the modularization offers protection to the cells, it also induces loss mechanisms that affect module power and energy yield. When a solar cell is integrated into a module, its working environment is altered (e.g. the glass and encapsulant layers introduce additional optical parasitic absorption), which affects its optical performance. Furthermore, the interconnection ribbons introduce additional resistive losses that affect the electrical performance. Because of the various loss mechanisms associated with the modularization process, the module power is generally less than the total of the power of all the individual cells used to fabricate the module. This difference between total cell power and module power is termed *cell-to-module (CTM) power loss.* The losses in the CTM process can be broadly separated into optical, resistive and mismatch components.

An accurate characterization of the CTM power loss (or gain) allows a better evaluation of new designs and materials in PV modules. The losses in the CTM process for wafer-based PV modules have been widely investigated by various researchers and module manufacturers [1–3]. To calculate the losses, solar cells and modules are typically measured using different *I–V* measurement systems, which consequently introduces uncertainty in the measurements [4].

> "An accurate characterization of the CTM power loss (or gain) allows a better evaluation of new designs and materials in PV modules."

To analyse the loss/gain in the CTM process more precisely, various measurement-based techniques are presented in this paper. These methodologies are easy to use and minimize the uncertainty in the CTM-loss/gain calculations. A quantitative analysis of the CTM loss/gain in silicon wafer-based PV modules is experimentally demonstrated.

Optical loss/gain in PV modules

For the light-harvesting analysis, a glass/backsheet PV module can be broadly divided into two parts: the active module area (i.e. containing the solar cells) and the backsheet area (i.e. without the solar cells).

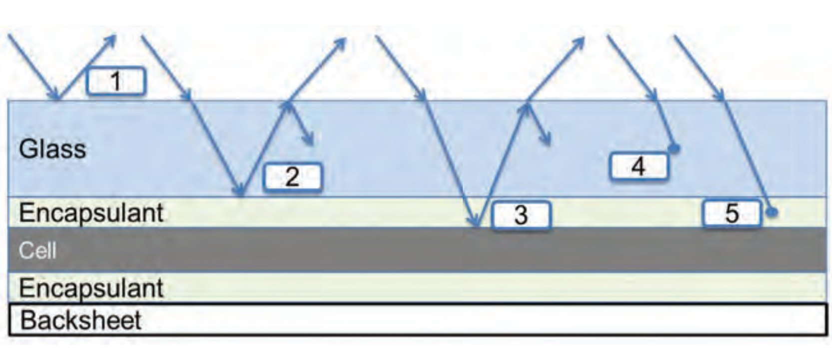

Figure 1. Optical losses in a silicon wafer-based PV module (active area). (Reflection: 1 = air–glass, 2 = glass–encapsulant, 3 = encapsulant–cell. Absorption: 4 = glass, 5 = encapsulant.)

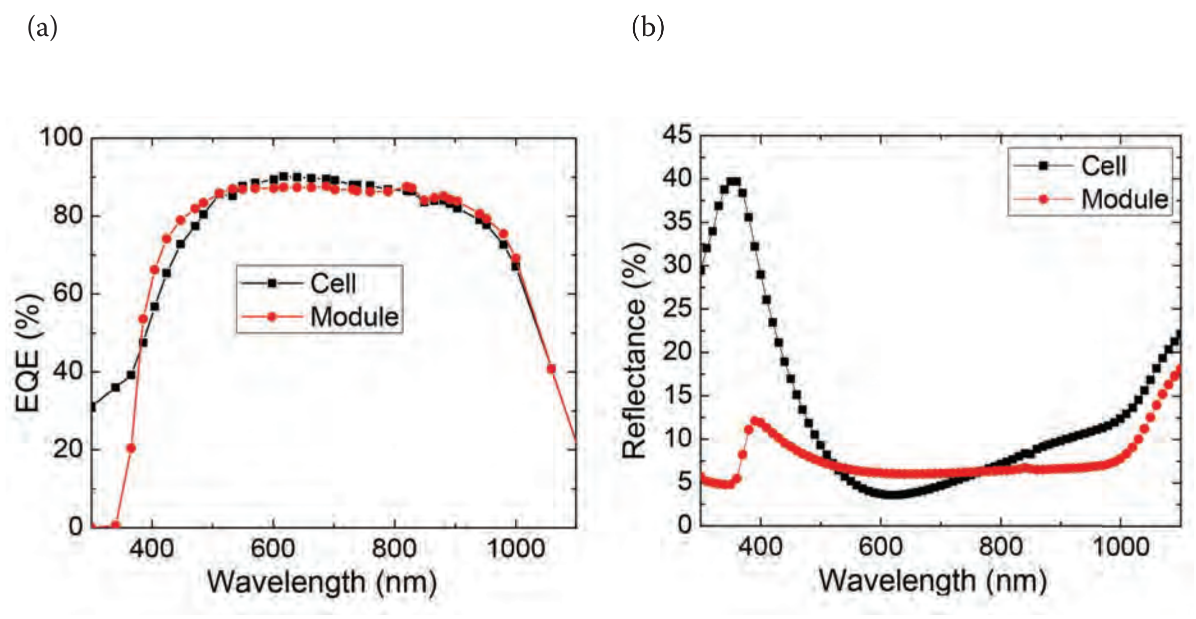

Figure 2. (a) Measured EQE of the cell and of the module with conventional EVA. (b) Corresponding reflectance measurements.

Power loss/gain for the active module area

Optical losses in the active module area occur because of the hemispherical reflectance at various interfaces and the parasitic absorptance of the encapsulation layers (glass, encapsulant) used to fabricate the module [5–7]. Fig. 1 shows the various optical loss mechanisms in a wafer-based PV module.

Besides the optical losses, there are also optical gains as a result of direct and indirect optical coupling. *Direct optical coupling* (reduced

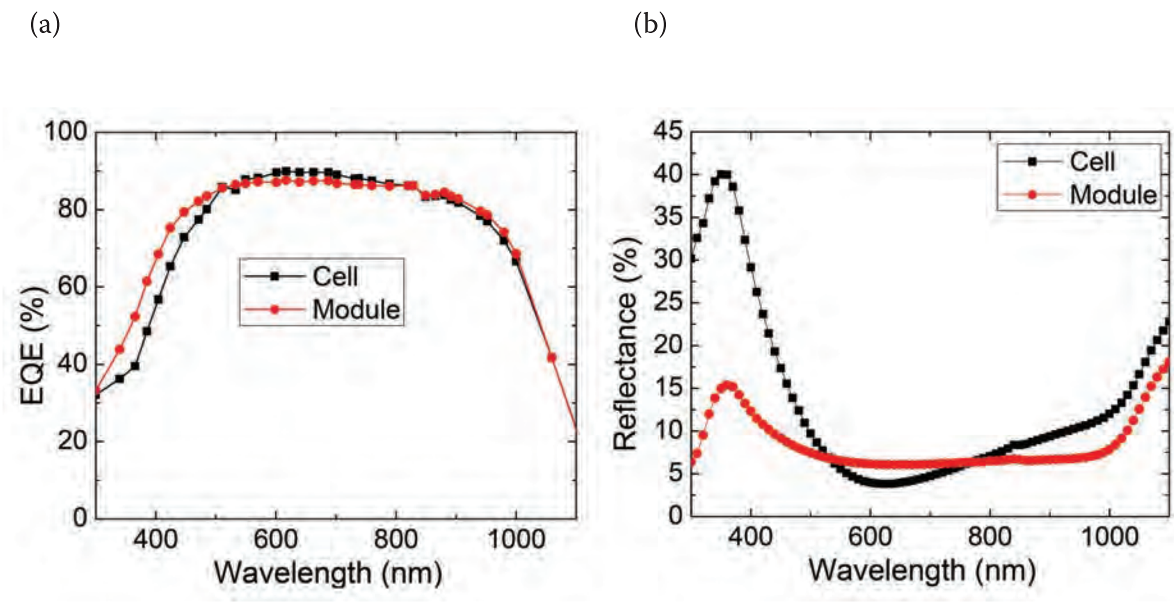

Figure 3. (a) Measured EQE of the cell and of the module with super-clear EVA. (b) Corresponding reflectance measurements.

reflectance) occurs because of the various encapsulation layers with monotonically increasing refractive indices [8–10]. *Indirect optical coupling* (reduced reflectance) occurs because of the total internal reflectance at the glass–air interface (from the contacting fingers and busbars), which redirects the light back onto the solar cell.

At SERIS, a method has been devised to experimentally quantify the optical loss resulting from parasitic absorption in the encapsulant materials (glass, EVA etc.), and the optical gain due to optical coupling [1]. The method requires the fabrication of single-cell mini-modules with a glass–glass configuration using processes and materials identical to those employed for large full-size modules. The glass–glass configuration can eliminate any edge effect caused by the backsheet around the cell area. The reflectance and the external quantum efficiency (EQE) of the bare solar cells and the mini-modules are measured using a UV-VIS and a full-area illumination EQE measurement system respectively.

Example: Comparison of different EVAs

To compare the parasitic absorptance losses in different EVAs, mini-modules with two different types of EVA were fabricated. The EQE and reflectance measurements were carried out on the solar cells before and after encapsulation, for two types of EVA, as shown in Figs. 2 and 3. With the

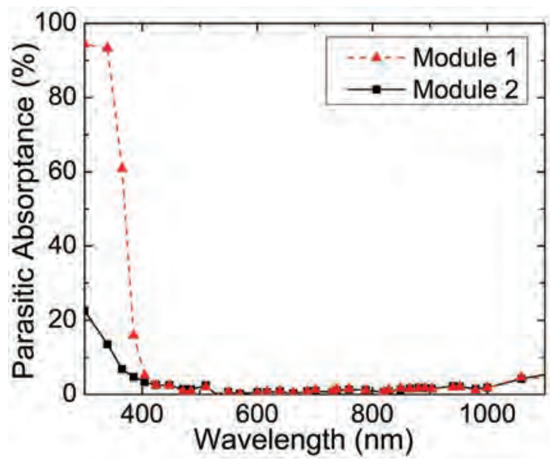

Figure 4. Parasitic absorptance for modules encapsulated with conventional EVA (module 1) and with super-clear EVA (module 2).

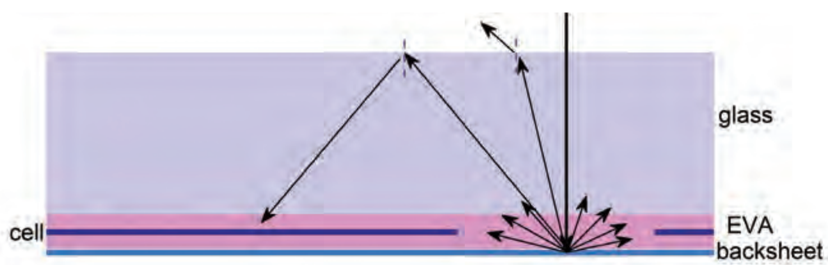

Figure 5. Schematic (not to scale) showing various light paths in a glass/backsheet PV module. Light incident on the cell-gap area of the backsheet is randomly scattered.

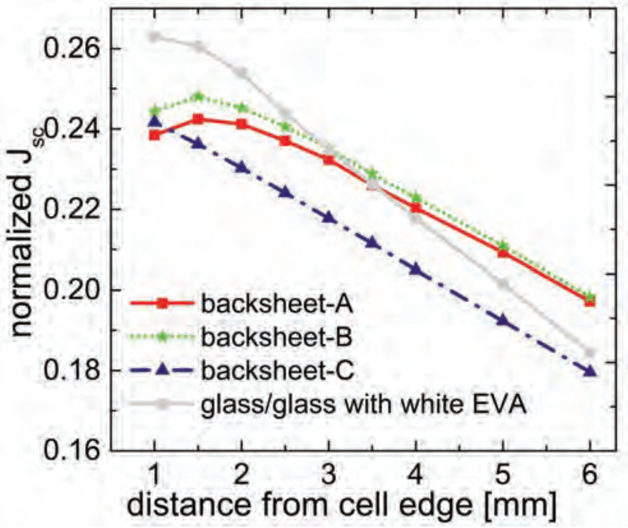

Figure 6. Normalized J_{sc} scans of mini-modules with different backsheets/EVA.

measurements taken from the bare cells and mini-modules, the parasitic absorptance A_{para} can be calculated [1] as:

$$A_{para} = 1 - R_{mod} - (1 - R_{cell}) \frac{EQE_{cell.mod}}{EQE_{cell}} \quad (1)$$

where R_{cell} and EQE_{cell} are the reflectance and EQE measured for the bare cell, while R_{mod} and $EQE_{cell.mod}$ are the measurements for the mini-module. The parasitic absorptance for the two modules with different EVAs is shown in Fig. 4.

The loss/gain in short-circuit current density (J_{sc}) can be calculated using the reflectance, parasitic absorptance data, and AM1.5G photon flux, and is summarized in Table 1. From this table it can be seen that after encapsulation, the cells encapsulated with conventional EVA lose an average of 0.39% of their J_{sc}, whereas the cells encapsulated with the super-clear EVA gain an average of 0.27% of their J_{sc}. The reason for this is that the modules encapsulated with super-clear EVA suffer less current loss due to parasitic absorption.

Power gain from the backsheet in the cell-gap area

In a conventional glass/backsheet module, the power gain is mainly due to the backsheet static concentration effect. The light incident onto the gap between the cells in a glass/backsheet module is scattered back at different angles. A significant proportion of this light can be entirely internally reflected at the glass–air interface and redirected onto the cells, thus increasing the module current. Fig. 5 illustrates this backsheet static concentration effect in a module. The gain in module current due to the backsheet is mainly influenced by the geometry of the backsheet area (cell-gap region), and by the backsheet properties (reflective and angular backscattering).

To quantify the current contribution due to the backsheet, an EQE line scan is performed on mini-modules (glass/backsheet). In this approach, EQE measurements are taken at several points (spaced at 0.5mm intervals) on the backsheet area, near the cell edge, using a small-area illumination source. The J_{sc} at each illumination point is then calculated from these EQE measurements and normalized with respect to the mini-module J_{sc} (measured on the cell area of the mini-module). An example of a plot of the normalized J_{sc} as a function of the distance of the illumination spot from the cell edge is shown in Fig. 6. The advantage of EQE line scan measurements is that the current gain for a module with a particular cell gap can be calculated directly, by integrating the normalized J_{sc} results.

Example: Comparison of different backsheets and white EVA

To evaluate the optical performance and associated current gain, three different types of backsheet and white EVA (glass/glass configuration) were compared. Mini-modules were fabricated using the different backsheets/EVA, and EQE measurements performed on these mini-modules. Fig. 6 shows the normalized J_{sc} plots for four different samples: for a module with a cell gap of 3mm and a string gap of 5mm, the current gain is calculated to be 2.14% (backsheet A), 2.20% (backsheet B), 2.08% (backsheet C) and 2.38% (white EVA).

Novel approach to quantifying light harvesting from the inactive area of a PV module

Besides the conventional approach of using EQE and spectrophotometry to quantify the optical properties of PV modules, SERIS has developed a novel method to quantify the light harvesting from the inactive area of a PV module using luminescence imaging [11]. Luminescence imaging, including electroluminescence (EL) and photoluminescence (PL), is a versatile technique for spatially resolved analysis of the optical and electrical properties of solar cells and modules. At SERIS, luminescence imaging has been demonstrated to be useful for spatially resolved optical characterization. This technique is used to access lateral variations of light harvesting in PV modules made of crystalline Si wafer solar cells. By exploiting the reciprocity theorem relating luminescence emission to EQE, a relative EQE map is extracted from a luminescence image of a PV module (see Fig. 7). In this way, the light-harvesting efficiency at the different inactive areas can be directly quantified.

Example: Comparison of different backsheets and light-redirecting film

To compare different backsheets and light-redirecting film using SERIS' new approach, several mini-modules were fabricated using different backsheets with and without light-redirecting film. Fig. 8(a) shows that for the mini-module with a white backsheet, more than 20% of the photons impinging on the backsheet near the cell edges are harvested. For the mini-module with the scattering tape, it can be seen that 45% of the photons impinging on the tape can be harvested. The scattering tape has the potential to be used in high-efficiency PV modules, as it is capable of harvesting

Module structure		Cell		Module			
		$J_{sc.Rcell}$ [mA/cm^2]	$J_{sc.cell}$ [mA/cm^2]	$J_{sc.Rmod}$ [mA/cm^2]	$J_{sc.Apara.mod}$ [mA/cm^2]	$J_{sc.mod}$ [mA/cm^2]	ΔJ_{sc} [%]
1	Glass/Conventional EVA/Tedlar	3.46	33.60	2.68	0.905	33.47	–0.39
2	Glass/Super-clear EVA/Tedlar	3.44	33.50	2.72	0.636	33.59	0.27

Table 1. Short-circuit current density and losses in short-circuit current density for modules with different types of EVA (AM1.5G spectrum).

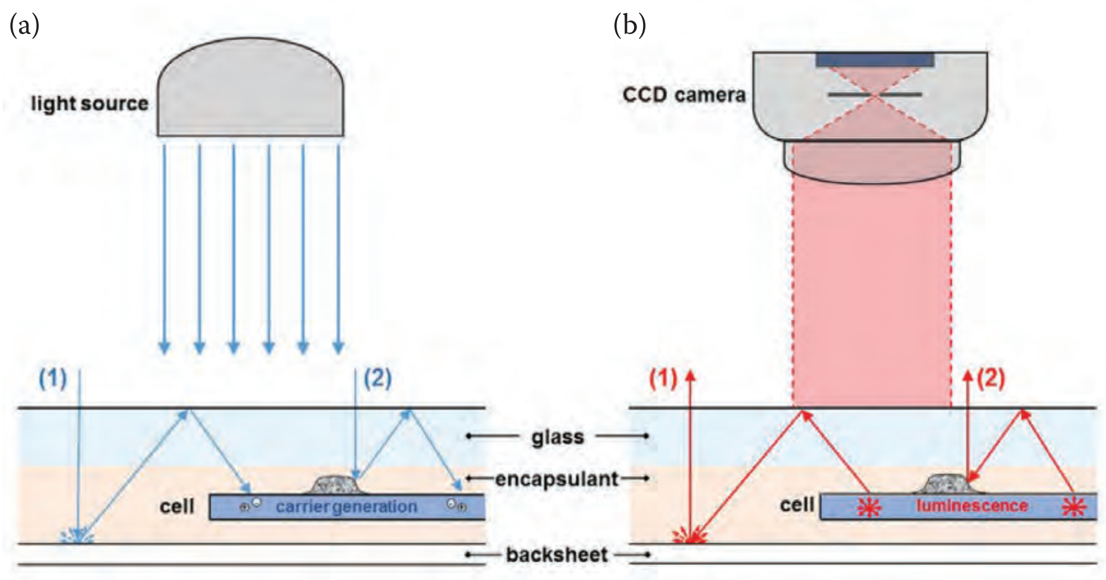

Figure 7. Schematic (not to scale) of the reciprocity relationship of (a) EQE measurement and (b) luminescence imaging. The solid lines with arrows labelled as paths 1 and 2 indicate the paths of the incident photons that are harvested by the cell, as well as the reverse paths of the emitted photons that are detected by the camera. Path 1 shows light harvesting from the backsheet area, while path 2 shows light harvesting from a metal finger.

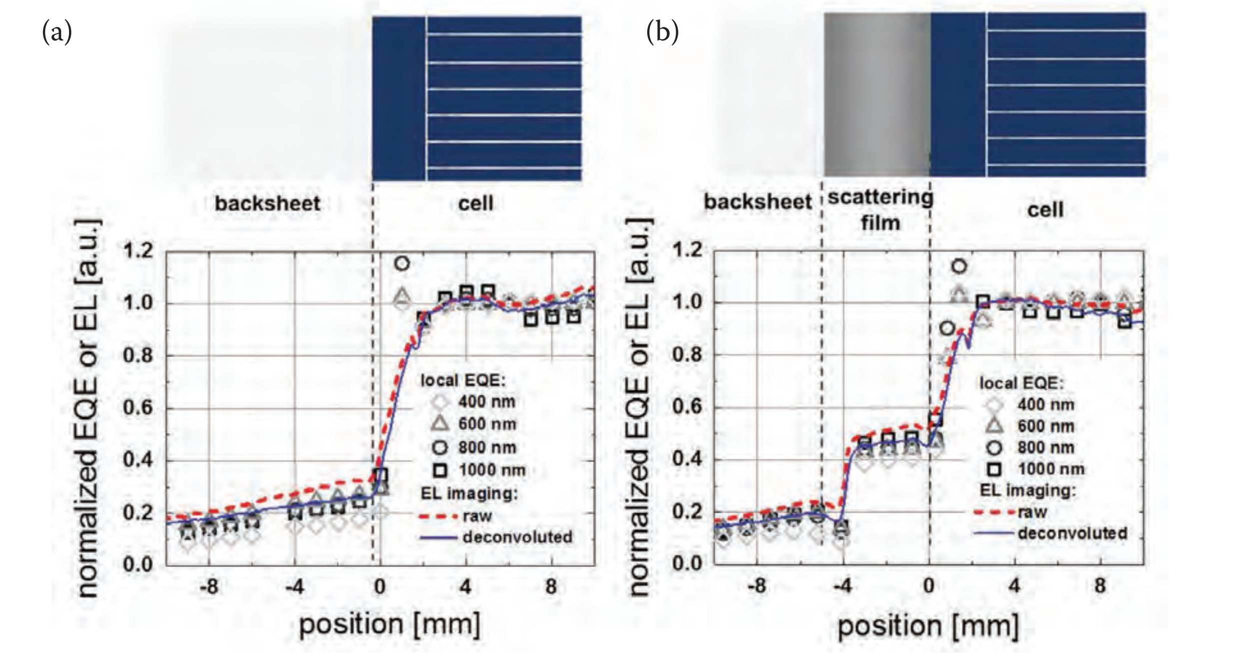

Figure 8. Line scan of the EL signal and local EQE near the cell edge of (a) a standard glass/backsheet mini-module, and (b) a glass/backsheet mini-module with additional scattering tape near the cell edge. Both EL and EQE data were normalized by the respective signals of the cell area. The EQE line scans are shown for 400, 600, 800 and 1000nm wavelengths.

more than twice the quantity of photons compared with the white backsheet. The light-harvesting efficiencies calculated using EL can then be translated to the relative gain in module current for a specific cell and string gap.

Power loss due to cell mismatch

Mismatch losses occur because of the difference in maximum power point currents (I_{mp}) of the individual series-connected solar cells [12]. If there is a difference in the I_{mp} of the cells, then the cells connected in series do not perform simultaneously at their individual maximum power points; this results in a total output power that is less than the sum of the maximum powers of individual cells [3]. PV module manufacturers deal with the mismatch by measuring and binning the solar cells prior to module fabrication [13].

To calculate the mismatch loss in a PV module, the individual cell's maximum power points and the maximum power point of a series interconnection of these cells must be known. Since in a finished module it is not possible to measure the operating point without the inclusion of optical and resistive effects, a combination of curve-fitting and circuit-simulation tools can be used to calculate the mismatch loss. The inputs to the simulation are the *I–V* curves of the individual solar cells, measured under standard test conditions (STC). Using curve-fitting and standard circuit-simulation software, such as LTSpice, the module *I–V* characteristics are determined on the assumption that the interconnection of the solar cells is ideal (i.e. there are no resistive losses due to cell interconnection). In this way, the simulated module *I–V* curve will provide the maximum power that accounts for mismatch losses only. The mismatch loss P_{mis} can be calculated using:

$$P_{mis} = \sum_{i=1}^{n} P^{i}_{cell} - P_{simu} \tag{2}$$

where P^{i}_{cell} and P_{simu} are the individual solar cell power and simulated module power respectively.

The mismatch loss was determined for the 60-cell modules incorporating two types of solar cell, namely n-type mono and p-type multi. The loss was calculated to be 0.14% for the n-type mono cells and 0.20% for the p-type multi cells.

Power loss due to resistive components

The resistive loss in a wafer-based PV module arises because of 1) the power losses in the various components used to interconnect the solar cells, and 2) the leakage currents at various points in the module. The main resistive components include the soldering ribbons, the bus ribbons, the contact resistance between the cell busbar and the soldering ribbons, the junction box and the cables; these are illustrated in Fig. 9, along with their relative contributions in a commercial 60-cell PV module. Resistive losses are a major concern for modules incorporating high-efficiency cells, particularly cells with improved current response [14].

To quantify the resistive loss in a 60-cell PV module, *I–V* measurements of individual cells are taken prior to module fabrication; the *I–V* characteristics of the finished module are then measured under STC. Because of the difference in cell and module measurement systems and their calibration standards, a certain amount of uncertainty is introduced in the measurements. To eliminate this uncertainty, the module *I–V* measurements are normalized with respect to the cell *I–V* measurements, or vice versa.

"Resistive losses are a major concern for modules incorporating high-efficiency cells."

In a module with solar cells connected in series, the short-circuit current of the module will be equal to the minimum of the short-circuit currents among the group of cells, corrected for the optical loss/gain. Similarly, the module open-circuit voltage will be equal to the sum of the open-circuit voltages of all the cells, provided that no cells are damaged as a result of the modularization process. Using the relative optical gain/loss P_{opt} calculated in the previous section, the normalized short-circuit current $I^{cal}_{sc.mod}$ and the normalized open-circuit voltage $V^{cal}_{oc.mod}$ of the module with respect to the cell measurements are given by:

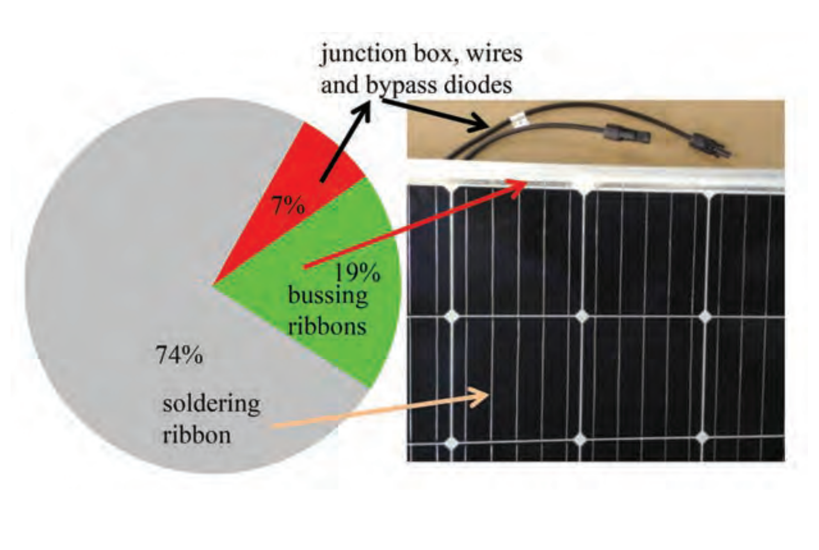

Figure 9. Additional resistive loss components in a PV module (over and above the solar cell series resistance).

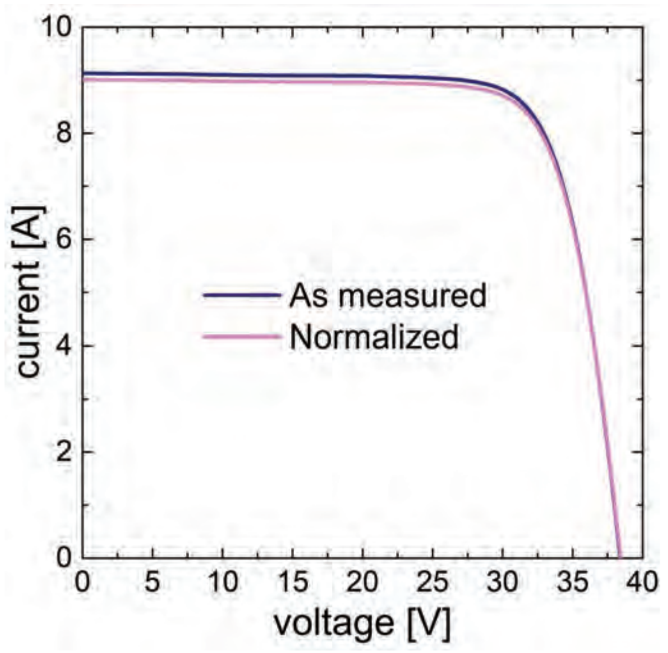

Figure 10. Module *I–V* curves: as-measured and normalized to solar cell measurements.

$$I^{cal}_{sc.mod} = (1 - P_{opt}) \min_{i=1} (I^{i}_{sc.cell})$$

$$V^{cal}_{oc.mod} = \sum_{i=1}^{n} V^{i}_{oc.cell} \tag{3}$$

The module I–V curve normalized using Equation 3 will be free from the errors caused by the cell and module measurements using two different systems. Fig. 10 shows the I–V curves, both as-measured and normalized to the cell measurements, for a module. The difference between the sum of the individual cell powers and the maximum power P^{norm}_{mod} of the normalized module I–V curve will be the total electrical loss (mismatch and resistive). Now, using the mismatch loss calculated earlier, the resistive loss in the CTM process can be obtained using the expression:

$$P_{res} = \sum_{i=1}^{n} P^{i}_{cell} - P^{norm}_{mod} - P_{mis} \tag{4}$$

Using the above analysis, the calculation of the resistive loss components for two 60-cell modules with n-type mono and p-type multi cells works out to be 4.7% and 4.1% respectively.

Module type	I_{sc} [A]	V_{oc} [V]	Fill factor [%]	Power [W]
p-type multi	8.84	37.90	77.5	259.6
n-type mono	9.13	38.39	76.8	269.2

Table 2. Measured electrical parameters for the two experimental modules.

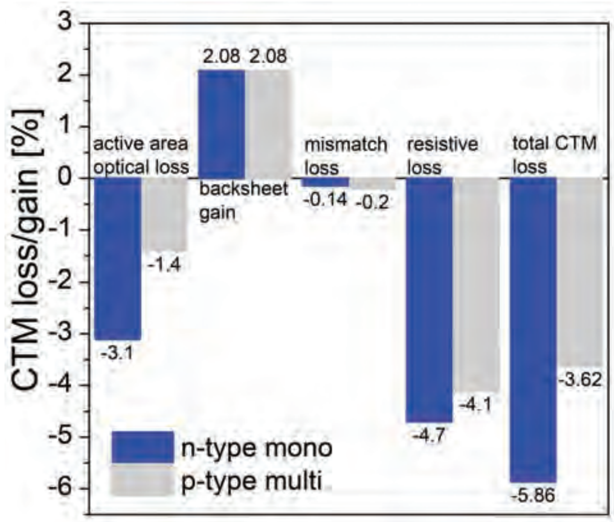

Figure 11. CTM power losses for p-type monocrystalline and n-type multicrystalline PV modules.

Discussion and conclusion

A CTM-loss calculation method has been demonstrated for two types of wafer-based module (60-cell) – one with monocrystalline cells and the other with multicrystalline cells. Table 2 lists the measured electrical parameters of the two types of module, while Fig. 11 shows a detailed chart of the CTM losses of the two module types.

In Fig. 11 it can be seen that mono cells have higher optical losses than multi cells when they are encapsulated into a module; the reason for this is that mono cells have better light absorption (less reflection) than multi cells, and hence the optical coupling gain is less for a mono cell. The mismatch losses do not contribute much to the total CTM loss and can therefore be neglected if a good cell-binning strategy is used. In the current experiments, the resistive losses are a major loss component: the losses obtained are on the high side, which indicates that the module interconnection process is not optimized. Some of the well-known technologies for reducing resistive losses in the CTM process are *half-cut cell* and *multi-busbar.*

"The mismatch losses do not contribute much to the total CTM loss and can therefore be neglected if a good cell-binning strategy is used."

An estimation and understanding of CTM losses in wafer-based PV modules is important, since these losses affect the energy yield of a module, and hence the cost of generated electricity. In this paper, various methods and equipment for quantifying the CTM losses/gains in a PV module have been presented. The calculations of individual loss components have been explained by experimental examples and the fabrication of mini-modules and large full-size modules. The presented analysis of CTM losses is important in helping module manufacturers to reduce the losses and improve module performance by carefully selecting the materials and optimizing the processes used in module fabrication.

References

[1] Khoo, Y.S., Walsh, T.M., Lu, F. & Aberle, A.G. 2012, "Method for quantifying optical parasitic absorptance loss of glass and encapsulant materials of silicon wafer based photovoltaic modules", *Sol. Energy Mater. Sol. Cells*, Vol. 102, pp. 153–158.

[2] Biao, L. et al. 2012, "Effect of encapsulant on cell-to-module efficiency loss in PV modules with ion implant and $POCl_3$ cells", *Proc. 38th IEEE PVSC*, Austin, Texas, USA, pp. 2336–2341.

[3] Wilson, K., De Ceuster, D. & Sinton, R.A. 2006, "Measuring the effect of cell mismatch on module output", *Proc. 4th WCPEC*, Waikoloa, Hawaii, USA, pp. 916–919.

[4] Spribille, A. et al. 2013, "HIP-MWT: Our approach for high performance ribbon based back contact MWT modules with low CTM losses", *Proc. 7th SNEC Int. PV Power Gen. Conf.*, Shanghai, China.

[5] Kang, M.H., Ryu, K., Upadhyaya, A. & Rohatgi, A. 2011, "Optimization of SiN AR coating for Si solar cells and modules through quantitative assessment of optical and efficiency loss mechanism", *Prog. Photovoltaics Res. Appl.*, Vol. 19, pp. 983–990.

[6] McIntosh, K.R. et al. 2009, "An optical comparison of silicone and EVA encapsulants for conventional silicon PV modules: A ray-tracing study", *Proc. 34th IEEE PVSC*, Philadelphia, Pennsylvania, USA, pp. 544–549.

[7] Peters, I.M., Yong Sheng, K. & Walsh, T.M. 2014, "Detailed current loss analysis for a PV module made with textured multicrystalline silicon wafer solar cells", *IEEE J. Photovolt.*, Vol. 4, pp. 585–593.

[8] Krauter, S. & Grunow, P. 2006, "Optical simulation to enhance PV module encapsulation", *Proc. 21st EU PVSEC*, Dresden, Germany, pp. 2065–2068.

[9] Haedrich, I. et al. 2013, "Minimizing the optical cell-to-module losses for MWT-modules", *Energy Procedia*, Vol. 38, pp. 355–361.

[10] Ballif, C., Dicker, J., Borchert, D. & Hofmann, T. 2004, "Solar glass with industrial porous SiO_2 antireflection coating: Measurements of photovoltaic module properties improvement and modelling of yearly energy yield gain", *Sol. Energy Mater. Sol. Cells*, Vol. 82, pp. 331–344.

[11] Z. Liu et al. 2016, "Luminescence imaging analysis of light harvesting from inactive areas in crystalline silicon PV modules", *Sol. Energy Mater. Sol. Cells*, Vol. 144, pp. 523–531.

[12] Bishop, J. 1988, "Computer simulation of the effects of electrical mismatches in photovoltaic cell interconnection circuits", *Solar Cells*, Vol. 25, pp. 73–89.

[13] Field, H. & Gabor, A.M. 2002, "Cell binning method analysis to minimize mismatch losses and performance variation in Si-based modules", *Proc. 29th IEEE PVSC*, New Orleans, Louisiana, USA, pp. 418–421.

[14] Guo, S. et al. 2013, "A quantitative analysis of photovoltaic modules using halved cells", *Int. J. Photoenergy*, Vol. 2013.

About the Authors

Jai Prakash Singh received his Ph.D. in electrical and computer engineering from NUS. He works as a research scientist at SERIS, where he focuses on characterization, loss analysis and optimization of c-Si solar cells and modules.

Yong Sheng Khoo has more than five years' experience in PV module development and testing, and is the head of the module development group at SERIS. He obtained his Ph.D. from NUS, and also has a B.S. and an M.Eng. in mechanical and aerospace engineering from Cornell University, USA.

Jing Chai received his MEngSc in photovoltaics from the University of New South Wales (UNSW), Australia, in 2010. Since 2012 he has been a research assistant at SERIS, where his research focus is on high-efficiency and long-durability Si-based PV modules.

Zhe Liu received a B.Eng. in electrical engineering from NUS in 2012. Since 2012 he has been a Ph.D. student at SERIS, with a research focus on modelling and characterization of Si solar cells and modules.

Yan Wang is the director of the PV module cluster at SERIS. He received his Ph.D. in 2007 through a co-educated graduate student collaboration between Forschungszentrum Jülich, Germany, and Nankai University, China.

Enquiries

SERIS
National University of Singapore
Block E3A, #06-01
7 Engineering Drive 1
Singapore

Tel: +65 660 11034
Email: yongshengkhoo@nus.edu.sg